

MODELLING OF ADVANCED III-V COMPOUND
SEMICONDUCTOR DEVICES

NIK NOR AMIRAH BINTI ROZIK

UNIVERSITI SAINS MALAYSIA

2017

MODELLING OF ADVANCED III-V COMPOUND
SEMICONDUCTOR DEVICES

By

NIK NOR AMIRAH BINTI ROZIK

Thesis submitted in partial fulfilment of the
requirements for the degree of
Bachelor of Engineering (Electronic Engineering)

JUNE 2017

ACKNOWLEDGEMENT

After undergone countless of efforts and discussions, Alhamdulillah praise to Allah for giving me strength and guidance to me in completing my final year project as partial fulfilment of the requirement to graduate. First and foremost, I would like to express my gratitude to my project's supervisor, Dr Mohamad Adzhar bin Md Zawawi for giving me suggestions and advices as well as encouragements along the project. This project would not be completed without the help from my supervisor.

Moreover, my special thanks to the authority of Universiti Sains Malaysia (USM) especially to School of Mechanical Engineering for providing me a chance to expose to the engineering field during my undergraduate programme. I have acquired myself with the knowledge and skills learnt from the courses provided in the school.

Next, I also would like to thank to my parents for always giving advice and encouragement whenever I have problems. Last but not least, I would like to thanks all the people who involved directly or indirectly in helping me during the project.

TABLE OF CONTENT

Acknowledgment	ii
Table of Contents	iii
List of Tables	vi
List of Figures	ix
List of Abbreviations	xii
Abstrakxiii
Abstract	xiv

Chapter 1: Introduction

1.1 Background	1
1.2 Problem Statement	2
1.3 Objectives of Research	2
1.4 Thesis Outline	3

Chapter 2: Literature Review

2.1 Introduction	5
2.2 Heterostructure.....	5
2.2.1 Band Discontinuities.....	6
2.2.2 Lattice Structure..	7
2.3 Basic Resonant Tunneling Diode	9
2.3.1 RTD Double Barrier Quantum Well.....	9
2.3.2 Theory and Operation of RTD.....	10
2.3.3 Theory of Electronic Transmission in RTD	12

2.4	Resonant Tunneling Diode: I-V Characteristic.....	15
2.5	Structural Parameter of RTD	17
2.5.1	Barrier Thickness	18
2.5.2	Spacer Thickness	19
2.5.3	Quantum Well Thickness	21

Chapter 3: Research Methodology

3.1	Introduction.....	23
3.2	Project Overview	23
3.3	Silvaco ATLAS.....	25
3.4	RTD model: GaAs/AlGaAs and InGaAs/AlAs	27
3.5	Non Equilibrium Green Function (NEGF).....	29
3.6	The Simulation: I-V Curve	29

Chapter 4: Results and Discussion

4.1	Introduction.....	31
4.2	Result Analysis.....	31
4.2.1	Default Thickness of GaAs/AlGaAs	32
4.3	Parameter Variations.....	36
4.3.1	Modelling with Barrier Thickness Variation.....	36
4.3.2	Modelling With Quantum Well Thickness Variations.....	39
4.3.3	Spacer Thickness Variations.....	42
4.3.4	Optimisation of GaAs/AlGaAs RTD Model.....	44

4.4 Default Thickness of InGaAs/AlAs	48
4.4.1 Modelling with Barrier Thickness Variation.....	52
4.4.2 Modelling with Quantum well Thickness Variation.....	55
4.4.3 Modelling with Spacer Thickness Variation.....	58
4.4.4 Optimisation of InGaAs/AlAs RTD Model.....	61
4.5 Summary.....	64
Chapter 5 : Conclusion And Future Work	
5.1 Introduction.....	65
5.2 Conclusion.....	65
5.3 Future Work.....	66
References	67
Appendix	70
GaAs/AlGaAs model RTD.....	70
InGaAs/AlAs model RTD.....	73

LIST OF TABLES

Table 3.1: Thickness parameters of GaAs/AlGaAs RTD model	28
Table 3.2: Thickness parameters of GaAs/AlGaAs RTD model.....	27
Table 4.1 Default Thickness of GaAs/AlGaAs RTD Model.....	32
Table 4.2: Comparison results obtained from I-V measured and simulated I-V curve of GaAs/AlGaAs RTD model.....	33
Table 4.3: Parameters for sample X.....	34
Table 4.3.1: Percentage difference of parameters between sample X and measured curve.....	35
Table 4.4: Parameter values for variations of barrier thickness for GaAs/AlGaAs RTD model.....	36
Table 4.5: I-V parameters output for samples X, A, B, C, and D.....	37
Table 4.6: Percentage difference for peak current and valley current for samples X, A, B, C, and D.....	38
Table 4.7: Percentage difference for peak voltage, valley voltage and PVCR for samples X, A, B, C, and D.....	38
Table 4.8: Parameter values for different quantum well thickness for GaAs/AlGaAs RTD model.....	39
Table 4.9: I-V parameters output for samples X, E, F, G and H.....	40
Table 4.10: Percentage difference for peak current and valley current for sample X, E, F, G and H.....	41
Table 4.11: Percentage difference for peak voltage, valley voltage and PVCR for sample X, E, F, G and H.....	41
Table 4.12: Parameter values for variations of spacer thickness for GaAs/AlGaAs RTD.....	42

Table 4.13: I-V parameters output for samples I, J, X, K and L.....	43
Table 4.14: Percentage difference for peak current and valley current for samples I, J, X, K and L.....	43
Table 4.15: Percentage difference for peak voltage, valley voltage and PVCR for samples I, J, X, K and L.....	44
Table 4.20: Parameters for Model Z.....	45
Table 4.21: Comparison results obtained from I-V measured GaAs/AlGaAs RTD model and simulated I-V curve GaAs/AlGaAs RTD model.....	46
Table 4.22: Band gap of simulated GaAs/AlGaAs RTD model Z.....	47
Table 4.23 Default Thickness of InGaAs/AlAs RTD Model.....	48
Table 4.24: Comparison results obtained from I-V measured InGaAs/AlAs RTD model and simulated I-V curve InGaAs/AlAs RTD model	49
Table 4.25: Parameters for sample Z.....	50
Table 4.26: Comparison results obtained from I-V measured InGaAs/AlAs RTD model and simulated I-V curve InGaAs/AlAs RTD model	51
Table 4.27: Parameter values for variations of barrier thickness for InGaAs/AlAs RTD model.....	52
Table 4.28: I-V parameters output for samples M1, M2, Z, M3 and M4.....	53
Table 4.29: Percentage difference for peak current and valley current for samples M1, M2, Z, M3 and M4.....	54
Table 4.30: Percentage difference for peak voltage, valley voltage and PVCR for samples M1, M2, Z, M3 and M4.....	54
Table 4.31: Parameter values for variations of quantum well thickness for InGaAs/AlAs RTD model.....	55
Table 4.32: I-V parameters output for samples Q1, Q2, Z, Q3 and Q4.....	56

Table 4.33: Percentage difference for peak current and valley current for samples Q1, Q2, Z, Q3 and Q4.....	57
Table 4.34: Percentage difference for peak voltage, valley voltage and PVCR for samples Q1, Q2, Z, Q3 and Q4.....	57
Table 4.35: Parameter values for variations of barrier thickness for InGaAs/AlAs RTD model.....	58
Table 4.36: I-V parameters output for samples S1, S2, Z, S3 and S4.....	59
Table 4.37: Percentage difference for peak current and valley current for samples S1, S2, Z, S3 and S4.....	60
Table 4.38: Percentage difference for peak voltage, valley voltage and PVCR for samples S1, S2, Z, S3 and S4.....	60
Table 4.39: Parameters for Model T.....	61
Table 4.40: Comparison results obtained from I-V measured InGaAs/AlAs RTD model and simulated I-V curve InGaAs/AlAs RTD model.....	62
Table 4.41: Band gap for simulated InGaAs/AlAs RTD model T.....	63

LIST OF FIGURES

Figure 2.1:Energy band diagram for 2 semiconductor before and after formation.....	6
Figure 2.2:Bandgap and lattice constant for various III–V and group-IV material alloys.....	7
Figure 2.3:Structural diagram of RTD.....	8
Figure 2.4:Schematic of quantum well with double barrier structure of RTD.....	10
Figure 2.5:The phenomena of quantum tunneling.....	11
Figure 2.6:Typical energy band of RTD under different bias voltage.....	12
Figure 2.7 (a):Transmission coefficient as function of incident energy (Emitter = 5 nm; collector = 5 nm).....	13
Figure 2.7 (b):Transmission coefficient as function of incident energy (Emitter = 5 nm; collector = 9 nm).....	13
Figure 2.7 (c) :Transmission coefficient as function of incident energy (Emitter = 5 nm; Collector = 15 nm).....	13
Figure 2.8 (a): Transmission coefficient as function of incident energy (Emitter = 5 nm; collector = 5 nm).....	14
Figure 2.8 (b):Transmission coefficient as function of incident energy (Emitter = 5 nm; collector = 9 nm).....	14
Figure 2.8 (c):Transmission coefficient as function of incident energy (Emitter = 5 nm; collector = 9 nm).....	14
Figure 2.9:I-V characteristics for a typical RTD.....	15
Figure 2.9.1: Another examples of different I-V characteristic obtained when different parameters were used. This example showed for different type of RTD model.....	16
Figure 2.10:Asymmetric DBRT structure for varied layer	17

Figure 2.11:Variable spacer layer samples and respectively measured current density.....	19
Figure 2.12:Typical I-V curve measured for variable width spacer layer samples.....	20
Figure 2.13: Schematic quantum well with finite double barrier structure.....	22
Figure 3.0: Flow chart of general idea how the process of the project.....	24
Figure 3.1: Silvaco simulation for inputs and outputs	25
Figure 3.1.1: Silvaco Inc.'s simulation environment.....	27
Figure 3.2: General stages of RTD simulation of XMBE66 and XMBE230.....	28
Figure 3.3: RTD I-V characteristic with parameter points.....	30
Figure 4.0: Results of measured GaAs/AlGaAs RTD model I-V curve vs with simulated I-V curve GaAs/AlGaAs RTD model.....	33
Figure 4.1: I-V curve comparison for sample X and measured curve.....	35
Figure 4.2: I-V curve characteristic for GaAs/AlGaAs RTD model with variation of barrier thickness.....	37
Figure 4.3: I-V curve characteristic for GaAs/AlGaAs RTD model with variation of quantum well thickness.....	40
Figure 4.4: I-V curve characteristic for GaAs/AlGaAs RTD model with variation of spacer thickness.....	43
Figure 4.5: Comparison I-V curve between measured curve/Sample X/Model Z.....	45
Figure 4.6: Band diagram of simulated GaAs/AlGaAs RTD model.....	47
Figure 4.7: Results of measured InGaAs/AlAs RTD model I-V curve vs with simulated I-V curve InGaAs/AlAs RTD model.....	48
Figure 4.8: I-V curve sample Z.....	50
Figure 4.9: I-V curve comparison for sample Z and measured curve.....	51

Figure 4.10: I-V curve characteristic for InGaAs/AlAs RTD model with variation of barrier thickness.....53

Figure 4.11: I-V curve characteristic for InGaAs/AlAs RTD model with variation of Quantum Well thickness.....56

Figure 4.12: I-V curve characteristic for InGaAs/AlAs RTD model with variation of Spacer thickness.....59

Figure 4.13: Comparison I-V curve between measured curve/Sample Z/Model T.....62

Figure 4.14: Band diagram of simulated InGaAs/AlAs RTD model.....63

LIST OF ABBREVIATIONS

RTD	Resonant Tunneling Diode
NDR	Negative Differential Resistance
PVCR	Peak-To-Valley Current Ratio
HEMTs	High Electron Mobility Transistors
MOSFET	Metal Oxide Field Effect Transistors
CMOS	Complementary Metal-Oxide-Semiconductor
DC	Direct Current
DBQW	Double Barrier Quantum Well
MBE	Molecular Beam Epitaxy
MOCVD	Metal-Organic Chemical Vapor Deposition
FWHM	Full-Width at Half-Maximum
TCAD	Technology Aided Computer Design
NEGF	Non-Equilibrium Green Function
QTBM	Quantum Transmitting Boundary Method

ABSTRAK

Diod salunan terowong (RTD) merupakan sejenis peranti elektronik yang telah dikaji dengan kerap oleh pelbagai penyelidik. Kekerapan ini adalah kerana peningkatan kepada permintaan dan keperluan kepada diod salunan terowong yang memiliki keupayaan untuk menanggung kekerapan yang berjumlah terahertz. Kelajuan kekerapan yang sangat tinggi daripada diod salunan terowong telah membolehkan penciptaan yang pelbagai untuk aplikasi dalam system komunikasi dan dalam pengimejan system untuk persekitaran penglihatan yang rendah. Diod salunan terowong berfungsi menggunakan quantum mekanikal bagi menghasilkan pengkamiran negatif. Fungsi projek ini dijalankan adalah untuk memahami mekanisma kaantum yang membolehkan RTD beroperasi. Selain itu juga, hubungan parameter fizikal RTD dan ciri-ciri I-V juga dikaji untuk lebih memahami sifat-sifat RTD. Seterusnya lengkungan I-V juga diselidik dan kesan perubahan parameter fizikal RTD kepada lengkungan I-V disiasat dengan lebih detail. Perisian simulasi Silvaco digunakan untuk menjalankan kajian keatas dua model RTD iaitu XMBE66 and XMBE230. Alat simulasi berdasarakan Tak Seimbang Fungsi Green (*Non-Equilibrium Green Function*, NEGF) yang menggunakan pendekatan masa berkesan telah digunakan dalam kuantum penghantaran simulasi ini. Simulasi ini juga dijalankan dengan model RTD yang berlainan lapisan epixatial untuk menyiasat kesan-kesan perubahannya keatas ciri-ciri I-V. Akhir sekali, kedua-dua ciri-ciri arus-voltan yang disimulasi dan ukuran RTD telah dibandingkan untuk mendapatkan penyesuaian yang terbaik dengan mengubah lapisan epilayer.

ABSTRACT

Resonant tunneling diode (RTD) is a type of electronic device that has been reviewed regularly by various researchers. The increasing in number of studying about RTD is because of increased demand and the need to resonant tunneling diodes that have the ability to bear the frequency of terahertz. The very high switching speeds frequency of the resonant tunneling diode has enabled the creation of a wide range of applications in the communication system and the imaging system for low-visibility environment. Resonant tunneling diodes using quantum mechanical works to produce a negative differential resistance (NDR). The function of this project is to understand the mechanism that allows RTD operates in quantum mechanical. In addition, the relationship of physical parameters and RTD I-V characteristics were also studied for a better understanding about the properties of RTD. The characteristics of I-V curves are also investigated and the effect of changes in the physical parameters of the RTD to the I-V graph is study in more details. Silvaco simulation software is used to carry out the studies on two model namely XMBE66 and XMBE230 RTD. A simulation tool based on Green function (Non-Equilibrium Green Function, NEGF) which use effective mass approach has been employed in this quantum transport simulation. This simulation model was also run with different layers epitaxial RTD to investigate the effects of the changes on the characteristics IV. Finally, both of the simulation and measured result of I-V graph were compared to get the best fit by varying the epilayer.

CHAPTER 1: INTRODUCTION

1.1 Background

The Resonant Tunnelling Diode (RTD) is a quantum well structure semiconductor device that uses electron tunnelling and has the unique property of negative differential resistance in its current-voltage characteristics. RTD started to receive great attention after it was first demonstrated by Chang, Esaki and Tsu in 1974 [1]. The resonant tunnelling diode (RTD) has been widely studied because of its importance in the field of nanoelectronic science and technology and its potential applications in very high speed/functionality devices and circuits where it can achieve a maximum frequency of up to 2.2 THz [2]. Some applications of resonant tunnelling diode (RTD) are high frequency oscillators, fast digital switches and devices for multiple valued logic which based on negative differential resistance (NDR) [3] .

The most common function of a diode is to allow an electric current to pass in one direction (called the forward biased condition) and to block the current in the opposite direction (the reverse biased condition). But, resonant tunnel diode (RTD) is a two terminal device and widely recognized as being inherently high speed device having a load I-V curve, characterized by a region of negative differential resistance. The diode is capable of generating a terahertz ($\times 10^{12}$ Hz) wave at room temperature[4].

The function of tunnelling diode is same as a CMOS transistor where the device will conduct current and turn the device on when there is specific external biased voltage is applied to the transistors. In CMOS transistor, current will goes through depletion region by tunnelling in normal tunnelling diodes while for RTDs, current will goes through quasi-bound states within it double barrier structure[2]. The most important design parameters for fabricating different devices are quantum wells and barriers of resonant tunnelling diodes [5].

1.2 Problem Statement

Resonant Tunnelling Diode exhibits I–V behaviour and it is very important as it will be very useful for implementation in many of the advanced and high speed applications [6]. For the following discussion, InGaAs/AlAs and GaAs/AlGaAs RTD will be used as the reference. RTDs have attracted a lot of attention because of their compatibility with many conventional technologies such for example a high electron mobility transistors (HEMTs) and metal oxide field effect transistors (MOSFETs) [2].

Many research has been done on the RTD devices including the structure and properties of the RTD model. However there are still lots of unexplored properties of RTD such as the relationship between physical variables of RTD and I-V characteristics. I-V characteristics are very useful for the implementation of RTD device and it will be affected by the changing of physical variables.

Several parameters are important for improving the performance of RTDs such as doping concentration of epitaxial process, the well width and size of the RTDs. To achieve a successfully performance for both of InGaAs/AlAs and GaAs/AlGaAs for high speed applications, simulation process using Silvaco can be conducted so that the optimum I-V characteristic can be achieved.

The modelling is stimulated in ATLAS SILVACO to extend the study of advanced III-V quantum devices. The Negative Differential Resistance (NDR) current and the peak-to-valley current ratio (PVCR) are simulated and validated with measurement data. Barrier thickness, quantum well thickness and spacer thickness are varies during simulation and the effect of varying parameters to the I-V characteristics are studied in order to obtain the best result.

1.2 Objectives

There are three objectives of this project:

1. To perform physical simulation on resonant tunnelling diode using Silvaco TCAD
2. To perform empirical I-V curve fitting in order to obtain the best fit
3. To determine the effect of barrier, spacer and quantum well thickness variation towards the I-V characteristics

1.4 Thesis Outline

This thesis consists of five main chapters that explain more details about this project. The first chapter is the introduction of the thesis where it gives background information about the topic and it also describe general idea about the project. It consist of the background, problems statement, objectives and thesis outline.

Chapter 2 is the literature review of the thesis. Basically it discussed about general idea and concept of principle operation of RTD. Some theories about quantum tunnelling mechanism are also being discussed. This chapter also covers the DC characteristics of RTD and effect of varying parameters to I-V characteristics.

Chapter 3 presents the methodology of the research where software development of this project is explain in detailed. The simulation software ATLAS SILVACO is explored in terms of method of operation and simulation.

Chapter 4 would be the results of the research. The result obtained from simulation of I-V curve using ATLAS are discussed effectively. The comparison between the measured result and simulated result obtained from the software will be compared and explained in order to prove the relation between the physical attributes and the I-V curve.

Lastly for chapter 5 it covers the conclusion of the thesis where it will summarize all the overall project work and achievements. In this chapter, the improvement that could be made for future work were also being described.

CHAPTER 2: LITERATURE REVIEW

2.1 Introduction

This chapter covers about project overview of the resonant tunnelling diode which divided into several sections in order to give basic knowledge about the topic.

This chapter starts with basic concept of RTD which are about heterostructures, band discontinuities and lattice structure of RTD. Besides that, the theory of operation of RTD also being reviewed in this section in order to gain related idea about the project. Structural parameters of RTD such as barrier thickness, spacer thickness, and quantum well thickness also included in the discussion. This chapter also give some review about I-V characteristics of RTD which known as negative differential resistance (NDR). The fundamental knowledge gained through this chapter are important in understanding further topic of this project.

2.2 Heterostructure

Heterostructures are the elements of many of the most advanced semiconductor devices presently being developed and produced. Heterostructure is defined as a semiconductor structure in which the chemical composition varies with position. The reason of investigation of semiconductor heterostructure is mainly to increase performance for multiple devices [7]. For example by using RTD oscillator a data transmission with rate of 3 Gbps at 540 GHz was demonstrated although the distance coverage was only a few centimeters due to the low oscillator output power [8]. The advantages of heterostructures is that they give precise control over the motion of charge carriers in semiconductor. The simplest heterostructure consist of a single heterojunction, but in most devices such as RTD there are two heterojunction thus it is better described as heterostructure.

2.2.1 Band Discontinuities

A junction occur when there are two semiconductors with different band gap are in contact, heterojunction or heterostructure will be formed [9]. Although doping influences heterojunction properties, the result of band gap different depends on different material types not the doping concentration. A discontinuity in the band diagram is caused by the difference of band gaps of two materials which it will affect the flow of carriers through the junction [9].

The difference the band gap of two semiconductor (for example narrow band gap InGaAs and wide band gap AlAs) forming a heterojunction which is unequally distributed between the valence band (E_V) and conduction band (E_C) [8]-[10].

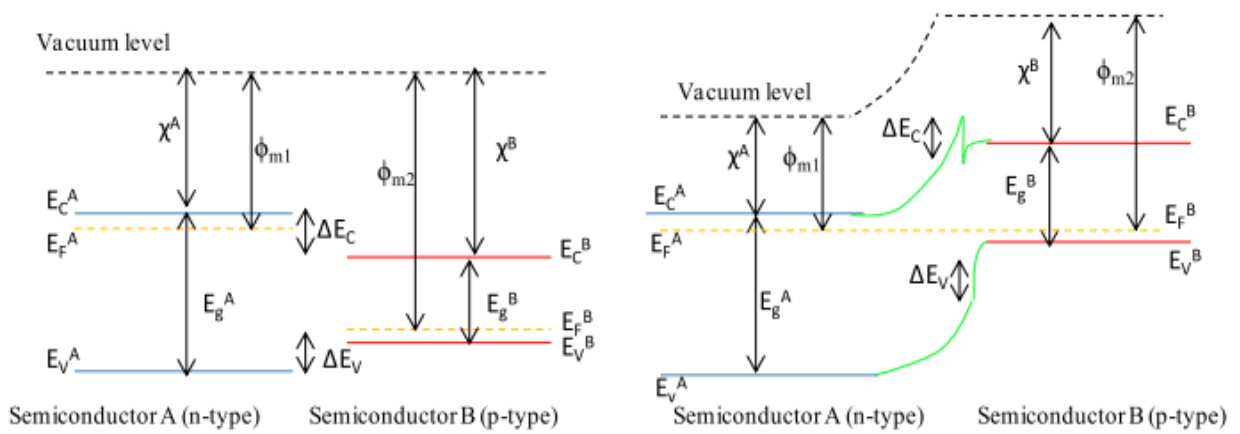


Figure 2.1: Energy band diagram for 2 semiconductor before and after formation [10]

Both semiconductor have valence band, E_V and conduction band, E_C while E_F refer to the Fermi level of semiconductor. Based on eq 2.1, total band gap discontinuity is

$$\Delta E_G = E_G^{(B)} - E_G^{(A)} \quad (\text{Eq. 2.1}) [11]$$

Where $E_G^{(B)}$ and $E_G^{(A)}$ are energy gap of each semiconductor respectively. The total discontinuity is divided between valence and conduction band discontinuity;

$$\Delta E_V^{(AB)} = E_V^{(A)} - E_V^{(B)} \quad (\text{Eq.2.2}) [11]$$

$$\Delta E_C^{(AB)} = E_C^{(B)} - E_C^{(A)} \quad (\text{Eq. 2.3}) [11]$$

Thus, the total discontinuity is the sum of valence band and conduction band;

$$\Delta E_G = E_V + E_C \quad (\text{Eq. 2.4}) [11]$$

2.2.2 Lattice Structure

Another factor that affect the modification of device characteristic and behaviours is the lattice structure of semiconductor materials. Although the formation of discontinuity creates freedom for engineer to modify RTD characteristics, it is essential to choose material pair with very close lattice constant in order to minimize the disturbance at heterojunction due to broken bonds in the interface [10].

Figure 2.2 shows the example of various band gaps and lattice constant for III-IV and group-IV materials. For example, both of GaAs and AlAs have lattice constant nearly the same which is as low as 1×10^{-3} and bandgaps that vary from 1.42eV to 2.1eV. While for $\text{In}_{0.8}\text{Ga}_{0.2}\text{As}$ material, the band gap was very narrow with 0.50 eV as compared to the lattice-matched $\text{In}_{0.53}\text{Ga}_{0.47}\text{As}$ material with 0.76 eV band gap [10].

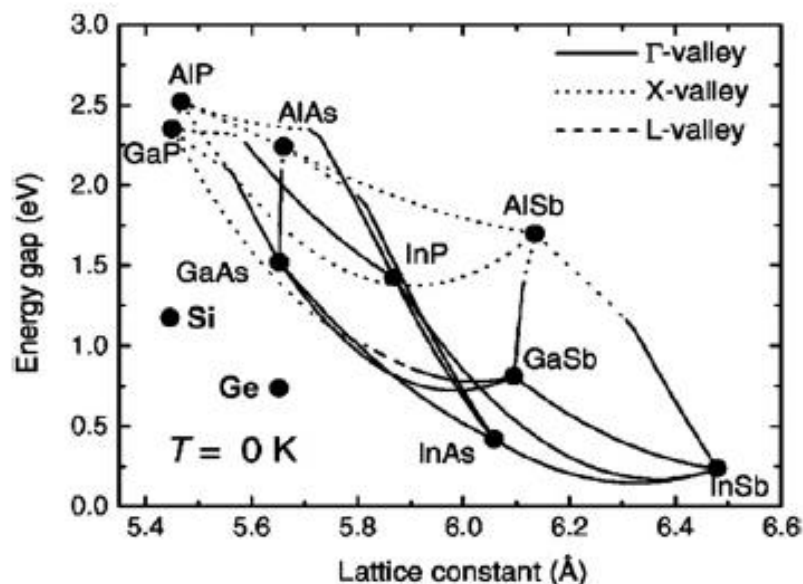


Figure 2.2: Band gap and lattice constant for various III–V and group-IV material alloys. [12]

For a high quality of heterojunction, lattice matched system is important and needed. To easily achieve lattice matched system, an alloy composition must be used especially the aluminium (Al) composition which is widely used in RTD model.

The most important region in heterostructure is the interface between two materials because poor quality of interface of materials will affect the potential advantages of these devices [13]. For example heterojunction with small lattice matched system but significant in bandgap for III-V semiconductor is InGaAs/AlAs and GaAs/AlGaAs. However other semiconductor still exists such as II-IV alloys, polycrystalline combinations of group-IV, II-IV, and/or III-V crystalline, microcrystalline, and amorphous semiconductors. The existing of different type semiconductor has increase the possibility for heterojunction formation in devices [10]- [12].

2.3 Basic Resonant Tunnelling Diode

The RTD mainly operates based on quantum mechanism where RTD utilize quantum well with same identically dopes contact and double barriers to achieve similar I-V characteristics [2].

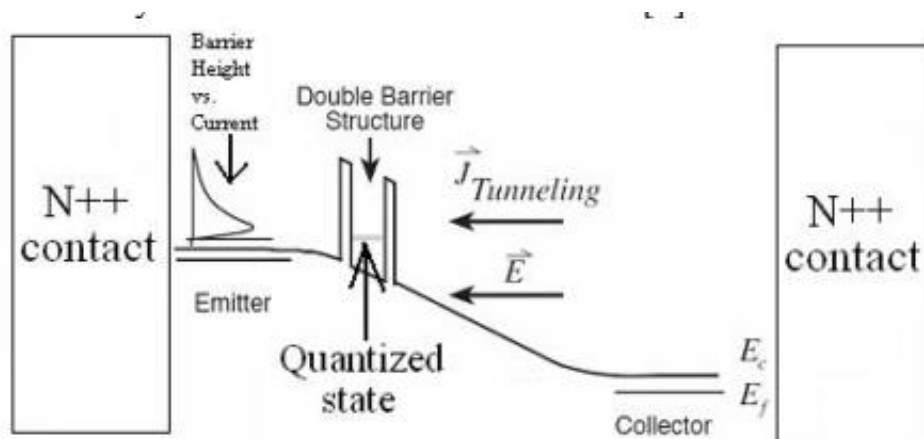


Figure 2.3: Structural diagram of RTD [2]

Based on figure above there are two types of doped contact; heavily doped, narrow energy-gap materials encompassing an emitter region, a quantum well between two barriers of

large band gap material and a collector region. The quantum well thickness is typically around 5nm with barrier layers range between 1.5 to 5 nm [14]. Furthermore, RTD also occurs at specific resonant energy levels with corresponding to the levels of doping and width of quantum well.

The electron flows in RTD are controlled by bias voltage. In order for the electrons to flow through the tunnel, the energy level of electrons in the source should match with quantized level in the well. Compared to TDs, RTD have great advantage because when a high reverse bias voltage is applied to TD, a leakage current occur. While for RTD, a symmetrical I-V response is produce when either forward bias or reverse bias voltage is applied [2].

2.3.1 RTD: Double Barrier Quantum Well

The basic configuration of RTD is called Double Barrier Quantum Well (DBQW) and it is the most common RTD structure as described by Sun et al [6]. DBQW is basically represented by an undoped semiconductor with smaller bandgap that acts as quantum well (also known as base) with two undoped barriers made with semiconductor. Along with the undoped semiconductors are the emitter and conductor which are heavily doped. Quantum phenomena such as interference, tunnelling and energy quantization are formed due to the comparison of the characteristics of the DBQW with the electron wavelength [6].

The layer between collector/emitter and DBQW is responsible for preventing the dopants on the collector/emitter layers to diffuse into DBQW. General features of the electron wave is produce by RTD as it traverse the DBQW thus resulting in the characteristic of RTD's called NDR.

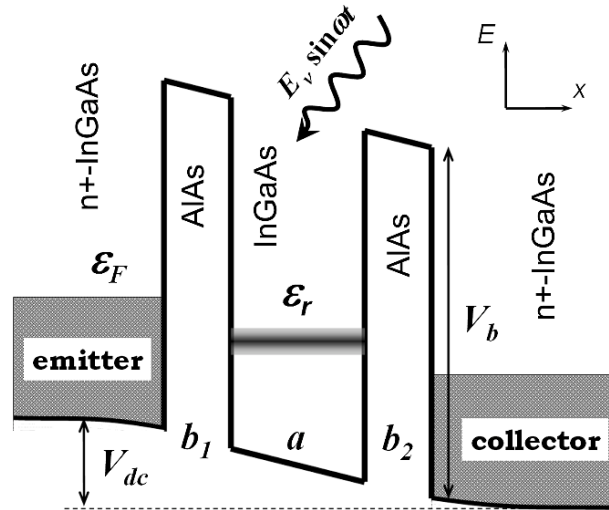


Figure 2.4: Schematic of quantum well with double barrier structure of RTD [15]

Each of InGaAs/AlAs and GaAs/AlGaAs are two terminals heterostructure device. For example of InGaAs/AlAs in figure 2.4 above, the emitter and collector contact region are heavily doped with n-type dopants.

2.3.2 Theory and operation of RTD

The fundamental theory that support RTD is the quantum tunnelling mechanism, it can produce unique property of negative differential resistance.

Quantum tunnelling that has no counterpart in classical physics is an important consequence of quantum mechanics. By considering a particle with energy E in the inner region of a one dimensional potential well $V(x)$ (potential that has lower value in certain region of space than in surrounding regions).

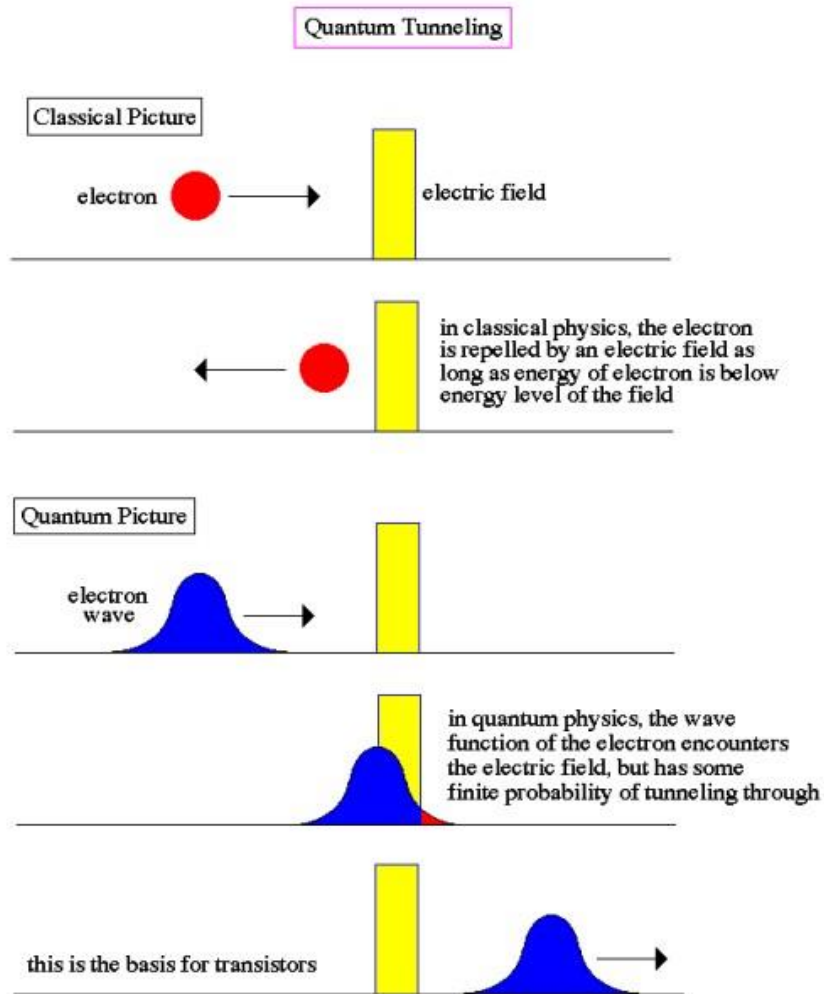


Figure 2.5: The phenomena of quantum tunnelling

Based on figure 2.5, for classical mechanics if the value of $E < V$ (the maximum height of the potential barrier), the particle remains in the well forever and cannot passing through the electric field unless it have sufficient kinetic energy to overcome the barrier. But for quantum mechanics view, the particle can easily escape if its energy E is below the height of the barrier V . The probability for the particle to escape is small unless E is close to V then the particle may tunnel through the potential barrier and emerge with the same energy, E [16].

In figure 2.6 the band structure of the RTD under different applied bias voltages is presented. RTD device consist of two tunnel barriers enclosing a quantum well. There are Fermi Sea of electron above the conduction band formed at the doped contact outside of the barriers. However, inside the well there are some resonant levels with some small width.

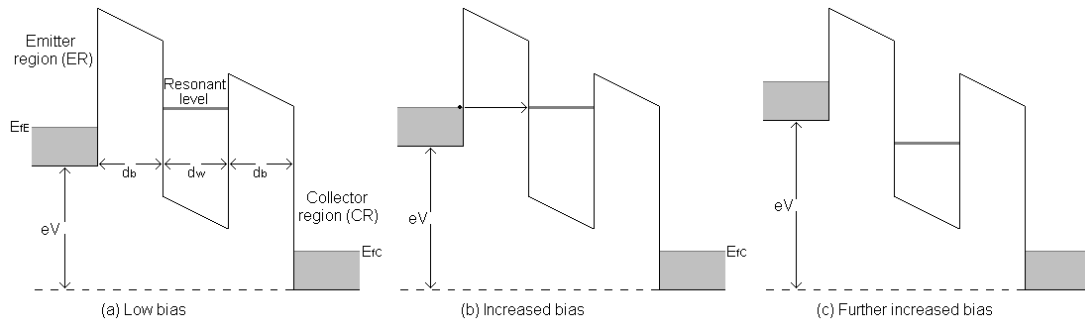


Figure 2.6: Typical energy band of RTD under different bias voltage

When low bias voltage is applied to the RTD (Figure 2.6(a)), a small current is produced due to non-resonant and scattering assisted tunnelling, leakage current through surface states and thermionic emission over the barriers. The emitter level rises relative to the resonant level as the bias voltage is increased. As the emission region conduction band is at same energy level of resonant level peak current is achieved (Figure 2.6(b)). NDR property is achieved when the resonant level falls below the emission region due to the further increasing value of voltage (Figure 2.6(c)). The flow of electrons across the Double Barrier Quantum Well (DBQW) are controlled by the external bias voltage, V .

2.3.3 Theory of Electronic Transmission in RTD

Research conducted showed that the resonant peaks of the trans-mission coefficients moved towards the lower energy regions as the applied bias voltage increases. The transmission coefficients displayed a numbers of resonant peaks and valleys. The first series of resonant peaks will attribute towards the resonant transmission through the fundamental quasi bound state. For the second series was due to the tunnelling through the first state. The transmission phenomena occurs when the energy of electron is close to the Eigen energy of the quantum well cased the wave function trapped in quantum well between the two barriers, reflecting back and forth between the emitter and collector regions so that a constructive interference will be produced [5].

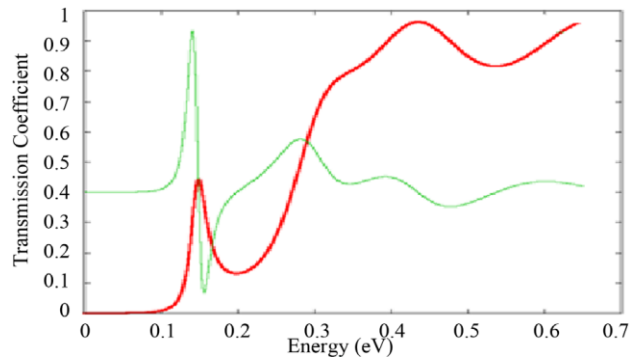


Figure 2.7 (a) Transmission coefficient as function of incident energy ($E_{\text{emitter}} = 5 \text{ nm}$;
 $collector = 5 \text{ nm}$) [5]

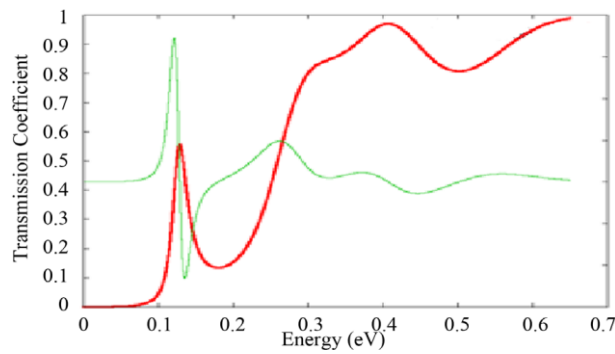


Figure 2.7 (b) Transmission coefficient as function of incident energy ($E_{\text{emitter}} = 5 \text{ nm}$;
 $collector = 9 \text{ nm}$) [5].

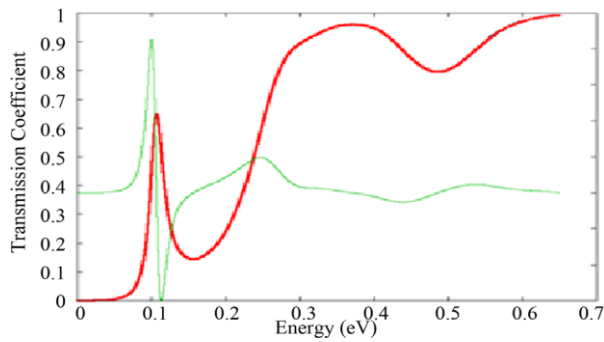


Figure 2.7 (c) Transmission coefficient as function of incident energy ($E_{\text{emitter}} = 5 \text{ nm}$;
 $Collector = 15 \text{ nm}$) [5].

Figure 2.7 (a-c) showed the effect of the emitter width on the transmission coefficient where the value for transmission coefficient increases with the thickness of the emitter.

Besides that, the maximum of the transmission coefficient for the first series also increasing when using the thicker collector. In figure 2.8 (a-b) it can be seen that the resonant peak moved towards higher energy as the thickness increases.

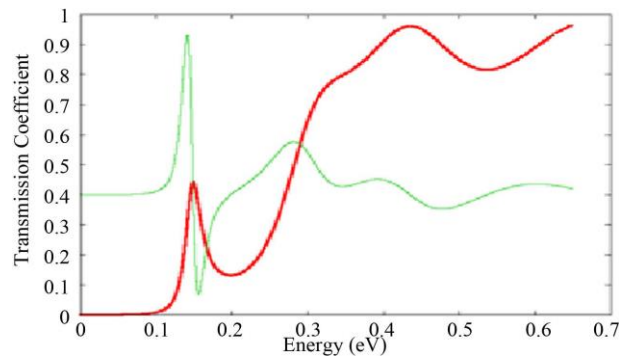


Figure 2.8 (a) Transmission coefficient as function of incident energy ($E_{\text{emitter}} = 5 \text{ nm}$; $collector = 5 \text{ nm}$) [5]

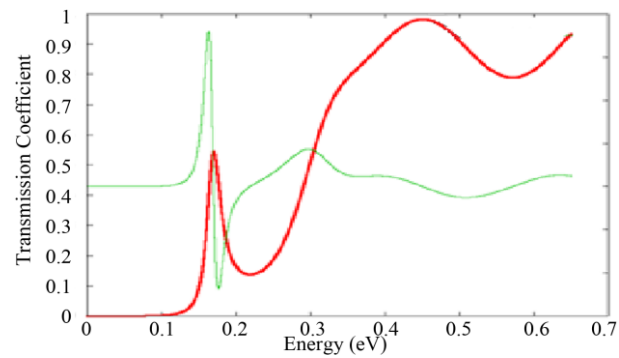


Figure 2.8 (b) Transmission coefficient as function of incident energy ($E_{\text{emitter}} = 5 \text{ nm}$; $collector = 9 \text{ nm}$) [5]

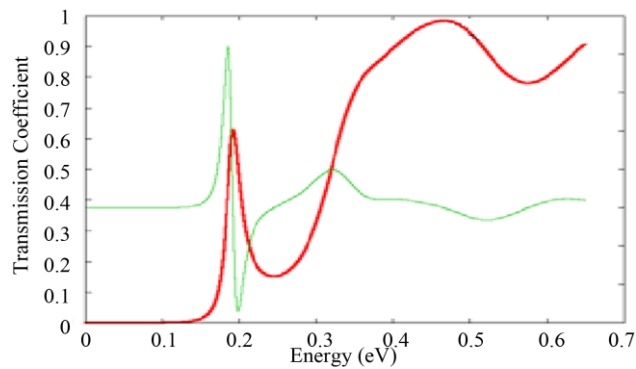


Figure 2.8 (c) Transmission coefficient as function of incident energy ($E_{\text{emitter}} = 5 \text{ nm}$; $collector = 9 \text{ nm}$) [5]

2.4 Resonant Tunnelling Diode: I-V Characteristics

The tunnelling effect of the RTD contributes towards exhibits I-V characteristics with a negative differential resistance (NDR) region. The resonant tunnelling diode (RTD) will be utilized mostly for the NDR based applications[17] .This phenomenon was first be done by Tsu and Esaki in the year 1973 [18]. Most important RTD property is that it can endure to a very high frequency and offers a very fast switching device. According to some research done, at frequency greater than 800GHz RTD can produce some small amounts of power and the calculation predicts that NDR response is in terahertz range [6].

Different type of current-voltage (I-V) curves with NDR characteristic by using different and suitable parameters [17]. The I-V curve of RTD is different compared to I-V curve of normal diode as in I-V curve of RTD contains a region where there is sudden drop in current .

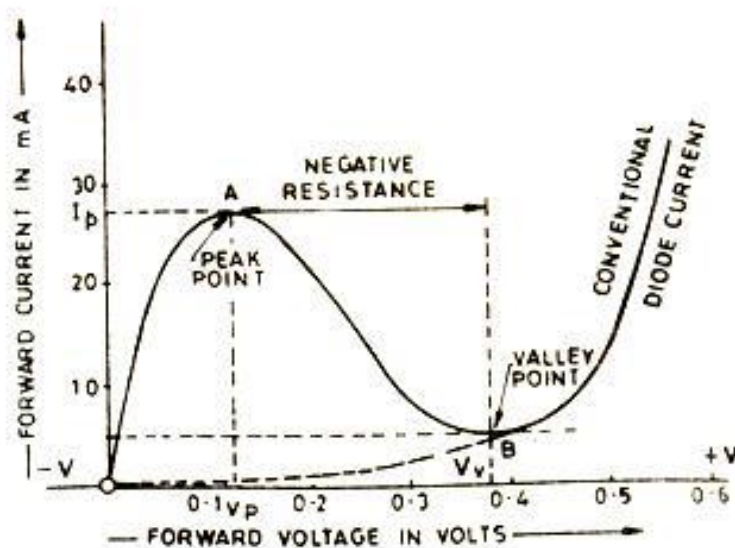


Figure 2.9: I-V characteristics for a typical RTD

I-V characteristic graph can be evaluated using several parameter such as peak-to-valley current ratio (PVCR). The resonant tunnelling mechanism have a greater peak-to-valley current ratio (PVCR) compared to conventional Esaki diode [19]. One of the most important

parameter that describing the quality of the resonant tunnelling diode is Peak-to-valley current ratio. However, it also can be a quite useless if the peak current obtained was too low [20]. The Peak-to-valley current ratio can be calculated using equation below

$$PVCR = \frac{I_p}{I_v} \quad (\text{Eq. 2.5}) [10]$$

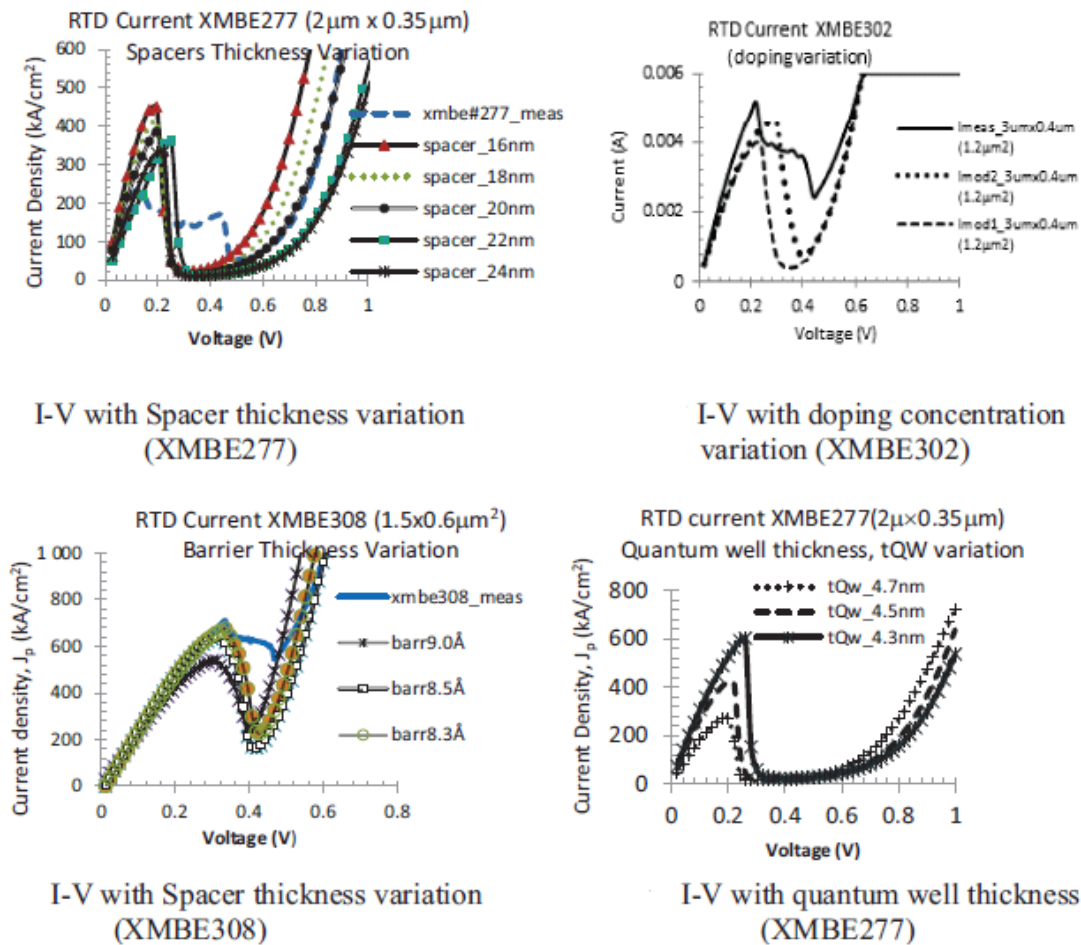


Figure 2.9.1: Another examples of different I-V characteristic obtained when different parameters were used. This example showed for different type of RTD model.

Figure 2.8, showed the effects of varying the spacer, barrier, quantum well thickness and doping concentration on the RTD current density. The relationship between spacer thickness and I-V characteristics for sample XMBE308 in figure above resulted in the undoped spacer prevent the diffusion of dopants to next layer during growth. For higher doping

concentration will produced an increment in peak current density, however it also caused a decrement in PVCR value due to an increase in peak current density which related to the leakage current as shown in figure 2.8 for doping concentration of XMBE302 device.

2.5 Structural Parameters of RTD

There are several types of material such as GaAs/AlGaAs [2], AlGaAn/GaAn/AlGaAn [21], InAs/GaSb/AlSb [22], InGaAs/AlAs [23] but for this project it covers InGaAs/AlAs and GaAs/AlGaAs. The physical structural parameters of RTD such as barrier thickness, t_b , spacer thickness, t_c , and quantum well thickness, t_{QW} can be change in order to optimise RTD performance [24]. Besides that, the selection of material also play an important role in obtaining the best performance of RTD because by choosing a proper material system, barrier heights, bandgap and the doping concentration can be controlled.

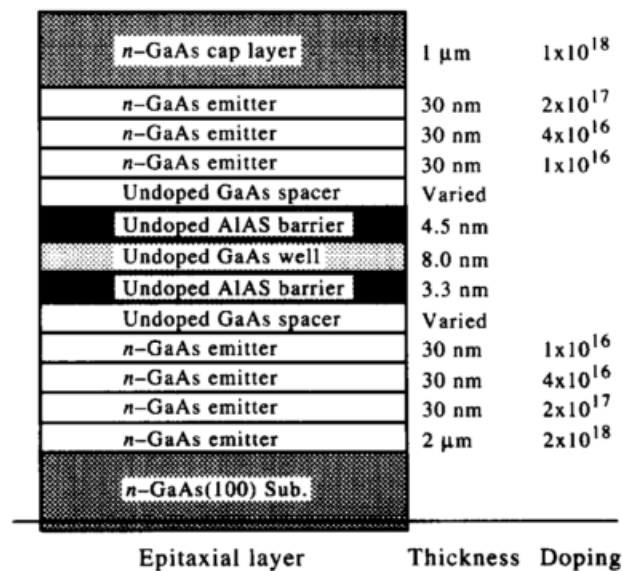


Figure 2.10: Asymmetric DBRT structure for varied layer [25]

2.5.1 Barrier Thickness

One of the most important relations in the operation of RTD is that current density, J is dependent on the barrier thickness, t_b [26]. The equation 2.60 shows expression for the tunnelling current in an RTD is given by the Tsu-Esaki formula:

$$J = \int_0^{\infty} T(E_z) S(E_z) dE_z \quad (2.60) [27]$$

$S(E_z)$ is the electron supply, E_z is electron energy component caused by momentum in the direction perpendicular to RTD barriers. For eq. 2.61 below shows the transmission probability

$$T(E_z) = \frac{m^{*L} k_z^L |A_{E_z}^R|^2}{m^{*R} k_z^R |A_{E_z}^L|^2} \quad (2.61) [27]$$

Where m^{*L} and m^{*R} refers to electron masses in the emitter and collector respectively, while for k_z^L and k_z^R are the electron wave numbers in the emitter and collector. For $A_{E_z}^R$ and $A_{E_z}^L$ means the transmission coefficients for an electron entering the left barrier from the emitter and exiting the right hand barrier into the collector [27]. Electrons pass through the barrier of RTD depends on a particular factor known as transmission probability, T as stated in equation;

$$T \alpha e^{-2Ktb} \quad (2.62) [24]$$

Where K is given by;

$$K = \sqrt{\frac{2m_b V}{h^2}} \quad (2.63) [24]$$

Where m_b refers to electron effective mass in barrier at energy which is close to the conduction band edge of emitter. Meanwhile h is reduced Plank Constant and V is potential barrier.

According to the equation 2.60 and 2.61, it's can be clearly seen that the transmission probability (T) increases as the current density (J) increases and decreasing barrier thickness, t_b . The peak voltage, V_p , increases with an increase in RTD current as a result of series resistance. However, Moise et.al stated that an increases in RTD is not significant as the variation of peak voltage in symmetrical barrier is more dominated by parasitic resistance [24].

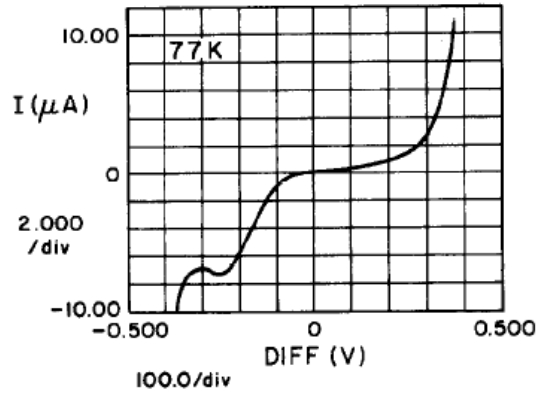
2.5.2 Spacer Thickness

Dopants are widely used in the formation of many structure od DBQW of RTD and it is important to use undoped spacer so that an electron mean free path (clear from ionised ion) can be formed.[24]. To make that happen, an undoped spacer must be included between the subsequent layers of the RTD model. Under applied bias, a triangle well will be formed at the area of contact barrier.

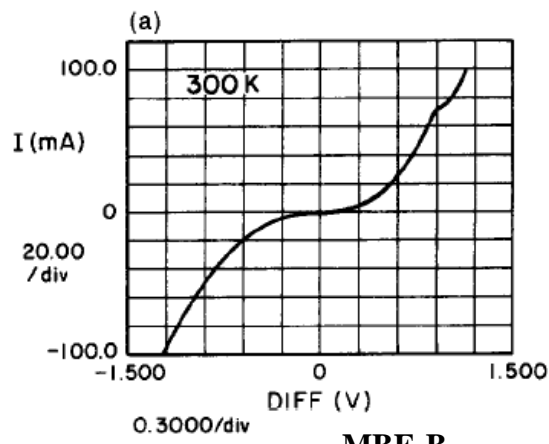
Sample #	L_{sp} (nm)	j_p (A/cm ²)
MBE-A	5	5.73×10^{-4}
MBE-B	10	9.29×10^{-4}
MBE-C	20	2.55×10^{-4}

Figure 2.11: Variable spacer layer samples and respectively measured current density [25]

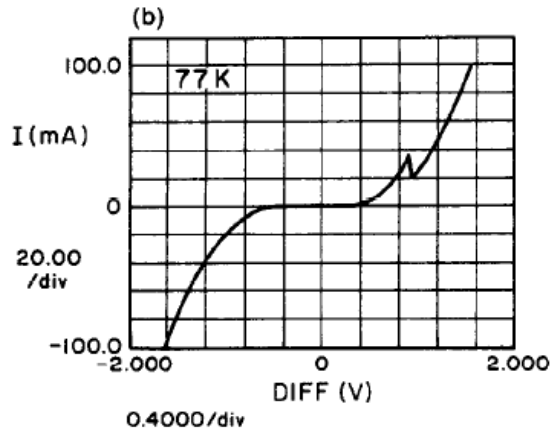
The previous research stated that the three samples types showed an increase in current density with the increasing spacer layer width until a certain threshold was reached ($L_{sp} > 10nm$). The transmission probability for RTD decreases exponentially as AlAs barriers become more asymmetric [25]. The I-V curve for the result are shown in figure 2.10.



MBE-A



MBE-B



MBE-C

Figure 2.12: Typical I-V curve measured for variable width spacer layer samples [25]

2.5.3 Quantum Well Thickness

Quantum wells are thin layered semiconductor structures that can be observed and controlled many quantum mechanical effects. There are two ways how quantum well structure can be grown which are molecular beam epitaxy (MBE) (Cho 1991), and metal-organic chemical vapour deposition (MOCVD) (Furuya and Miramoto 1990). These technique can achieve a layer thickness control to about one atomic layer [28].

A very high peak current densities are required for high frequency operation so that the maximum power available from the RTD can be obtained. This can be done by decreasing the thickness of the quantum well barrier and also increasing the emitter doping level [2].

The equation of quantisation energy off quantum well is

$$E_n = \left(\frac{\hbar^2 \pi^2}{2m_w t_w^2} \right) n^2 \quad (2.70) [10]$$

Where m_w and t_w are the electron effective mass inside the quantum well and the thickness of the quantum well respectively.

Decreasing the quantum well thickness can caused the first resonant energy level to increases. This phenomena will be needed a bias voltage that produce peak current to increases thus the peak voltage is also push to a higher value [10]. The reduction in quantum well thickness also will decrease PVCR and increase the valley current producing more power consumption due to increased leakage current [2].

According to the Wentzel-Kramers-Brillouin (WKB) approximation, the full-width at half-maximum (FWHM) of the nth resonant level is;

$$\Delta E_n = E_n \exp\left(-2t_b \sqrt{\frac{2m_b(V_0 - E_n)}{\hbar^2}}\right) \quad (2.71) [10]$$

Where E_n denotes quantisation energy, t_b is barrier thickness, m_b denotes electron effective mass in barrier, V_0 denotes barrier height and \hbar denotes reduced Plank constant.

Increases in ΔE_n will cause in increasing the transmission coefficient $T(E)$, thus it will shifted the resonant tunnelling current to a higher value.

$$T(E) = \frac{4T_{lb}T_{rb}}{(T_{lb} + T_{rb})^2} \left[1 + \left(\frac{E - E_n}{\frac{1}{2}\Delta E_n}\right)\right]^{-1} \quad (2.72) [10]$$

Figure 2.9.3 below shows the quantisation energy in the quantum well E_n increases with reduction in electron effective mass, m_w as well as a reduction in quantum well thickness, t_w .

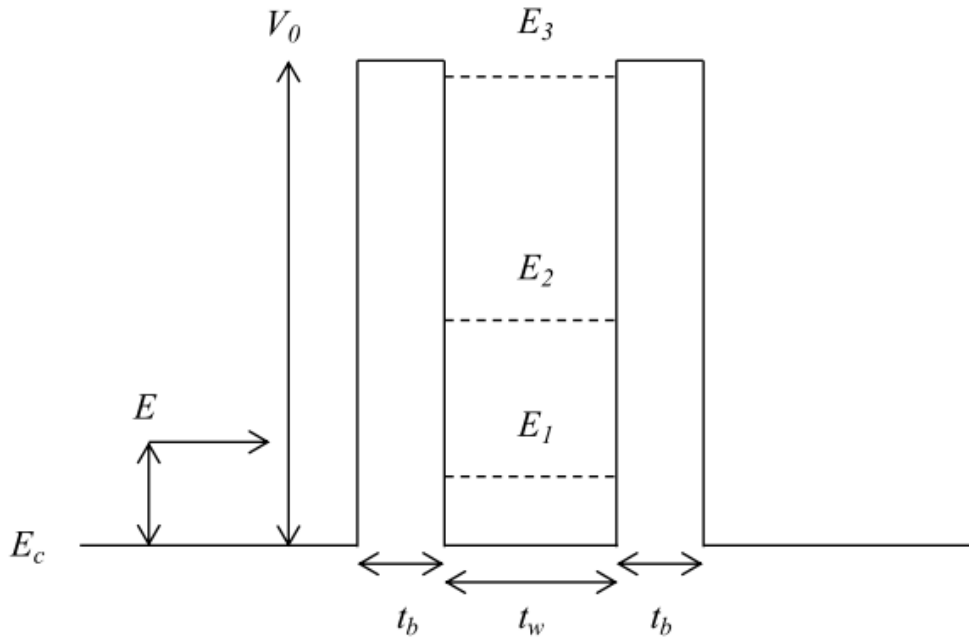


Figure 2.13: Schematic quantum well with finite double barrier structure

CHAPTER 3: METHODOLOGY

3.1 Introduction

This chapter presented an outline on research of methodology used in simulate the physical characteristic both of InGaAs/AlAs and GaAs/AlGaAs. Silvaco ATLAS simulator will be used in this project to simulate the desire I-V curve. For the first section in this chapter, a general information about this software were presented. Next section is about steps involve in simulating and modelling the choosen RTD choose. It will discuss the flow of whole process in order to give details explanation about this project.

1.2 Project Overview

Before proceed to the simulation of the InGaAs/AlAs and GaAs/AlGaAs, some literatures review were done for collected fundamental about this topic. The epilayer structure of default GaAs/AlGaAs and InGaAs/AlAs of RTD was used for simulation of SILVACO ATLAS. Through this simulation, the physical simulation obtained is compared to the measured result and the difference of I-V characteristic graph between both results is analysed. The physical parameters that played an important role in determined the I-V characteristic graph is barrier thickness, quantum well thickness and spacer thickness. These physical parameters will be varied until the best fit was obtained. A series of simulation was done to obtain several different I-V curves which reflects different scenarios.

The difference between measured value and simulated value must be in the acceptable range which should not greater than 20% which can be considered good for margin error [10]. This is really important because if the range is greater than 20%, it will affect the overall RTD I-V graph. Below is the equation that can use to calculate percentage different;

$$\text{Percentage different (\%)} = \frac{\text{simulation result} - \text{measured result}}{\text{measured result}} \times 100\% < 20\%$$

Figure 3 summarise the general idea how the process of competed the project was done. Before the simulation was done, some reading about the theory of RTD and information about GaAs/AlGaAs and InGaAs/AlAs is gathered together. Then the comparison between the results and analysis was conducted in order to identify the relationship of the variations of parameters with I-V characteristics.

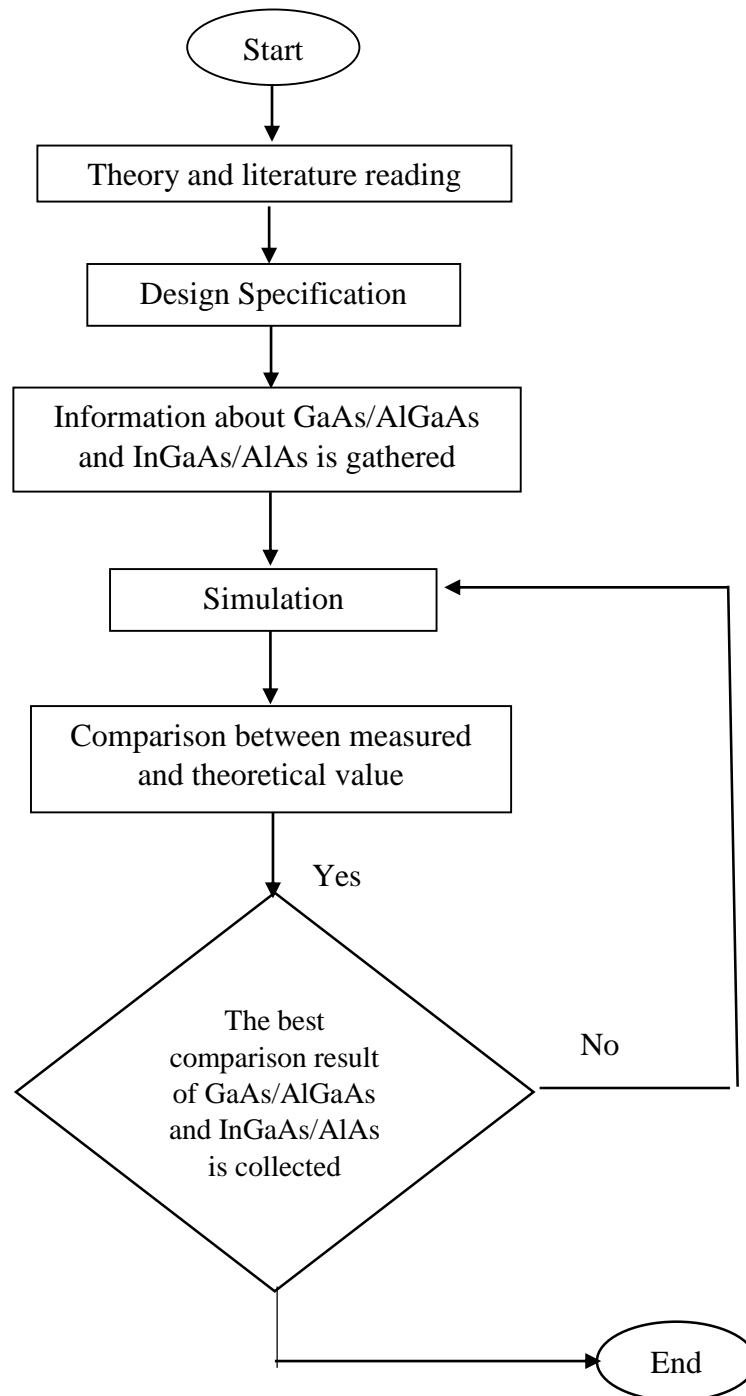


Figure 3.0: Flow chart of general idea how the process of the project